

X-Ray Raman Scattering in Metals*

S. Doniach

Applied Physics Department, Stanford University, Stanford, California 94305

and

P. M. Platzman

Bell Telephone Laboratories, Murray Hill, New Jersey 07974

and

J. T. Yue†

Physics Department, Stanford University, Stanford, California 94305

(Received 13 May 1971)

It is shown that new information about the many-body singularities at the soft x-ray absorption edge in metals could be obtained from an x-ray Raman experiment in which the energy dependence of the edge is observed as a function of momentum transfer (scattering angle). For Li, in particular, it is predicted that a dramatic change could occur from a many-body inhibition of the edge at small scattering angles to an enhancement of the edge at larger scattering angles.

I. INTRODUCTION

In the last few years the soft x-ray emission and absorption spectrum resulting from conduction-band core-state transitions in metals has come under intensive theoretical analysis. While the problem of this spectrum in simple metals such as Li and Na is an old one, early attempts to explain the experimental results were based exclusively on a one-electron picture of the solid.¹ This one-electron approach has not been entirely successful in explaining some of the observed experimental structures in the spectrum.^{2,3} More recently Mahan and Nozières and co-workers^{4,5} have shown that many-body final-state interactions can produce qualitative changes in the shape of the soft x-ray absorption and emission edges in metals resulting from the scattering of Fermi-surface electrons from the core-state hole.

Which of the approaches to the interpretation of soft x-ray spectra in simple metals is more correct? Are the observed anomalies due to many-body effects? In this paper we propose an experiment which could yield additional information about the physics of the transitions involved in the soft x-ray experiments and hence help to pin down the correct interpretation.

The experiment we propose is based on an x-ray Raman effect in which the photon ($\hbar\omega_1 \cong 10$ keV) excites a core electron up to the Fermi level and is scattered through some angle θ with a "small" corresponding energy loss $\hbar\omega$. This scattering is diagrammed schematically in Fig. 1.

Such an inelastic scattering phenomenon, as we will show, provides additional information to a straight soft x-ray emission or absorption experi-

ment. The additional information is gained through the fact that the scattering leads to an appreciable momentum transfer \vec{q} , i. e., the scattering cross section is a function of

$$\vec{q} = \vec{k}_2 - \vec{k}_1 \quad (1)$$

and

$$\omega = \omega_2 - \omega_1. \quad (2)$$

More precisely,

$$\frac{d\sigma}{d\Omega d\omega} \sim S(\vec{q}, \omega). \quad (3)$$

In the limit of small angle (i. e., forward) scattering, we will in fact show that the energy dependence of $S(\vec{q}, \omega)$ simply reduces to that of the direct x-ray absorption experiment. However, as the angle is increased and one changes the momentum transfer \vec{q} , we will show that different scattering phase shifts for the scattering of Fermi-surface electrons from the core hole dominates the form of the many-body threshold singularity and that the resulting "spectrum" (as a function of ω) may be expected to change if these effects are important.

II. MANY-BODY EFFECTS IN SOFT X-RAY EMISSION AND ABSORPTION

Before going on to a discussion of the Raman process, we summarize in this section the theory of the "simple" soft x-ray absorption process.

In excitation from a core state to the conduction band the probability is given, in the one-electron picture, to lowest order in the electromagnetic field, by the usual Golden Rule formula

$$P(\omega) \sim \sum_{\vec{k}, n} |\langle \Psi_{\vec{k}, n} | \vec{p} \cdot \vec{A} | \varphi \rangle|^2 \delta(\omega - E_k - E_{\text{core}}), \quad (4)$$

where \vec{p} is the momentum of the electron and $\vec{A} = \vec{e}(2\pi\omega)^{-1/2} e^{i(\vec{q}\cdot\vec{r} - \omega t)}$ is the vector potential of the electromagnetic wave. The wave function φ is the core-electron function and $\Psi_{\vec{k},n}$ the corresponding conduction-band state with crystal momentum \vec{k} and band index n . The bandwidth at the core states, whose energy is E_{core} below the conduction band, is taken to be zero. In a soft x-ray experiment, the wave vector \vec{q} of the photon is essentially zero, i. e., the wavelength of the few-hundred eV x rays is extremely long relative to typical atomic distances and the vector potential \vec{A} may be taken to be the constant polarization vector \vec{e} of the field.

In the absence of any band-structure effects the wave function is a plane wave and we may evaluate Eq. (4) exactly. If φ is a hydrogenic state, then the matrix element in Eq. (4) selects out the p -wave character in $\Psi_{\vec{k}}$ and

$$P(\omega) \sim \omega^{3/2} \text{ for } \omega > E_{\text{edge}}, \quad (5)$$

where $E_{\text{edge}} = E_{\text{core}} + E_{\text{Fermi}}$.

This simple one-electron picture is modified by several effects.

- (i) The plane-wave conduction-band state should be replaced by a suitable Bloch wave, still a one-electron effect.
- (ii) The interaction between the conduction electrons and the infinitely heavy hole should be included in the matrix element.
- (iii) The interaction between conduction electrons should also be included.

Originally Mahan⁴ and later Nozières and co-workers⁵ showed that the interaction between the deep hole and the electrons in the conduction band had a profound effect on the shape of the spectrum near threshold. They neglected complications (i) and (iii) (arguing that they were unessential) and found that (ii) led to a singular behavior near threshold ($\omega = E_{\text{edge}}$) of a form given by

$$P(\omega) \sim \sum_l \frac{W_l(\omega)}{(\omega - E_{\text{edge}})^{\alpha_l}}, \quad (6)$$

with

$$\alpha_l = 2\delta_l/\pi - \alpha$$

and

$$\alpha = 2 \sum_l (2l+1)(\delta_l/\pi)^2. \quad (7)$$

The phase shift δ_l characterizes the scattering of conduction electrons at the Fermi surface from a hole in a state of relative angular momentum l . The quantity $W_l(\omega)$ represents a matrix element which is slowly varying with respect to the frequency ω . From an s -state core the matrix element $W_l(\omega)$ only exists for $l=1$, i. e., the photon in the dipole approximation supplies an angular momentum of 1 to the core electrons.

In Li metal, in which the core state is in the K shell, the experiments seem to show that an inhibition of $P(\omega)$ occurs near the emission edge.² Several authors have produced arguments based on the assumption that the form of this spectrum is still one electron in character, i. e., that this inhibition arises from band-structure effects.¹ The alternative (and somewhat more intriguing) explanation is that this inhibition is due to the many-body effects described by Eq. (6). As pointed out by Ausman and Glick,⁶ this can result from $\alpha_1 < 0$ in Eq. (6). A negative α_1 seems to be consistent with their calculation of the phase shift based on scattering from a screened Coulomb potential. For $l=0$, on the other hand, as occurs for instance in the L -shell emission spectrum in Na, Ausman and Glick point out that one expects $\alpha_0 > 0$, with the result that the threshold should be enhanced in this case (as is seen experimentally).³

In the Sec. III we show that the Raman experiment can provide a direct test of this interpretation of the threshold inhibition in Li by allowing measurement at nonzero momentum transfer.

III. THEORY OF THE RAMAN PROCESS

Several authors⁷ have shown that, for nonrelativistic x rays, the cross section for Raman scattering can be written down directly in terms of the charge density correlation function for the metal, i. e.,

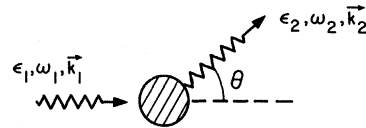
$$\frac{d\sigma}{d\Omega d\omega} \sim S(\vec{q}, \omega), \quad (8)$$

where

$$\begin{aligned} S(\vec{q}, \omega) &= 2\pi \sum_f \left| \langle f | \sum_j e^{i\vec{q}\cdot\vec{r}_j} | i \rangle \right|^2 \delta(E_f - E_i - \omega) \\ &= \int_{-\infty}^{\infty} \langle \rho_{\vec{q}}(t) \rho_{-\vec{q}}(0) \rangle e^{i\omega t} dt \end{aligned} \quad (9)$$

is the electronic structure factor and

$$\rho_{\vec{q}} = \int e^{i\vec{q}\cdot\vec{r}} \rho(\vec{r}) d^3r \quad (10)$$



$$\omega = \omega_1 - \omega_2 \quad (\text{ENERGY TRANSFER})$$

$$\vec{q} = \vec{k}_1 - \vec{k}_2 \quad (\text{MOMENTUM TRANSFER})$$

$$\frac{d\sigma}{d\omega d\Omega} = \left(\frac{d\sigma}{d\Omega} \right)_0 S(\vec{q}, \omega)$$

FIG. 1. Energy and momentum transfer in x-ray Raman scattering.

is the Fourier transform of the electronic charge density of the ground state. Equation (9) is similar to Eq. (4) except insofar as the matrix element contains $e^{i\vec{q}\cdot\vec{r}}$ instead of the quantity $\vec{p}\cdot\vec{A}$. Since $\vec{q}\cdot\vec{r}$ can be varied by changing the scattering angle (unlike the soft x-ray absorption case), the scattered spectrum involves all powers of qr instead of just the linear term.

What kind of additional information is contained in Eq. (9)? At the energy transfer of interest (corresponding to the core conduction-band transition) the density operator may be written as

$$\rho(\vec{r}) \cong \sum_i \sum_{\vec{k}} \Psi_{\vec{k}}^*(\vec{r}) \varphi_i(\vec{r}) c_{\vec{k}}^\dagger a_i + \text{H. c.}, \quad (11)$$

where $\Psi_{\vec{k}}(r)$ is the Bloch function for an electron in state k and φ_i is the core-state wave function on the i th atom and $c_{\vec{k}}^\dagger$ and a_i are the corresponding electron and hole creation operators. Assuming that the core states are tightly bound, Eq. (9) may now be written (per atom) as

$$S(\vec{q}, \omega) = \sum_{\vec{k}, \vec{k}'} M_{\vec{k}}(\vec{q}) M_{\vec{k}'}(\vec{q}) R(\vec{k}, \vec{k}', \omega), \quad (12)$$

where

$$R(\vec{k}, \vec{k}', \omega) = \int_{-\infty}^{\infty} dt e^{i\omega t} \langle c_{\vec{k}}^\dagger(t) a(t) a^\dagger(0) c_{\vec{k}'}(0) \rangle \quad (13)$$

contains all the many-body effects and

$$M_{\vec{k}}(\vec{q}) = \int d^3r_1 \Psi_{\vec{k}}^*(\vec{r}_1) \varphi(\vec{r}_1) e^{i\vec{q}\cdot\vec{r}_1} \quad (14)$$

is the matrix element for the scattering process from a single atom. Since the core states are by definition orthogonal to the valence band, we see that in the limit $q \rightarrow 0$,

$$M_{\vec{k}}(\vec{q}) = 0. \quad (15)$$

The Mahan-Nozières model^{4,5} for calculating the correlation function used in Eq. (13) assumes the electrons to be noninteracting with one another, and with the periodic lattice potential, the hole to be infinitely heavy and the interaction between the electron and hole to be described by a central potential $V(r)$, i. e.,

$$H_{\text{int}} = \sum_{\vec{k}, \vec{k}'} V_i(k, k') Y_{lm}^*(\hat{k}) Y_{lm}(\hat{k}') c_{\vec{k}}^\dagger c_{\vec{k}'} a^\dagger a. \quad (16)$$

The quantity $V_i(k, k')$, when the conduction-band wave functions are plane waves, is simply given by

$$V_i(k, k') = (2l+1) \int j_l(kr) j_l(k'r) V(r) r^2 dr. \quad (17)$$

In order to simplify the calculations somewhat, it has generally been assumed that these quantities are independent of k and k' , i. e., that V_i leads to a description of the scattering in terms of the energy independent phase shifts δ_l .

In this model the time dependence of the correlation function matrix (k and k') is diagonalized by projecting the plane wave $\Psi_{\vec{k}}$ onto a given spherical wave mode, i. e.,

$$R(\vec{k}, \vec{k}', \omega) = \sum_{lm} Y_{lm}(\hat{k}) Y_{lm}^*(\hat{k}') \bar{R}_l(\omega). \quad (18)$$

For ω near threshold, the quantity $\bar{R}_l(\omega)$ is given by

$$\bar{R}_l(\omega) = 1/(\omega - E_{\text{edge}})^{\alpha_l}, \quad (19)$$

with α_l given by Eq. (7).

In Li the quantity $\varphi(r)$ is the bound s -state core wave function. Substituting Eqs. (18) and (19) into Eq. (12) we find that the Raman cross section in the threshold region is given by

$$S(\vec{q}, \omega) = \sum_l A_l(\vec{q}) \bar{R}_l(\omega), \quad (20)$$

where

$$A_l(\vec{q}) = \sum_m |(4\pi)^2 \int r^2 dr j_l(k_F r) j_l(qr) \varphi^*(r) Y_{lm}(\hat{q}) - (4\pi)^{3/2} \delta_{m,0} \delta_{l,0} |\varphi(r)|^2 \tilde{\varphi}(k_F) j_0(qr)|^2 \quad (21)$$

and

$$\tilde{\varphi}(q) = \int d^3r e^{i\vec{q}\cdot\vec{r}} \varphi(r). \quad (22)$$

In Eq. (21) the second term in the integral arises

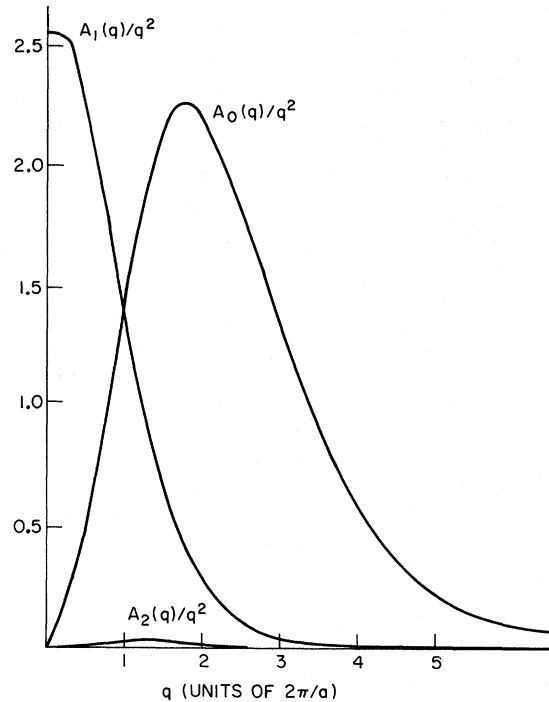


FIG. 2. Dependence of matrix elements $A_l(\vec{q})$ Eq. (20) as a function of momentum transfer \vec{q} in units of $2\pi/a$. The core wave function was taken to be of hydrogenic form $\varphi_{\text{core}}(r) = (\lambda^3/\pi)^{1/2} e^{-\lambda r}$ with $\lambda = 1/a_{\text{Li}}$ and $a_{\text{Li}} = 0.371$ Bohr radius. The function $A_1(q)/q^2$ is plotted to show the relation to the x-ray absorption at small Raman scattering angles (small q). a is the atomic cell distance for Li crystal (3.50 Å). λ on this scale ($2\pi/a = 1$) is 2.84.

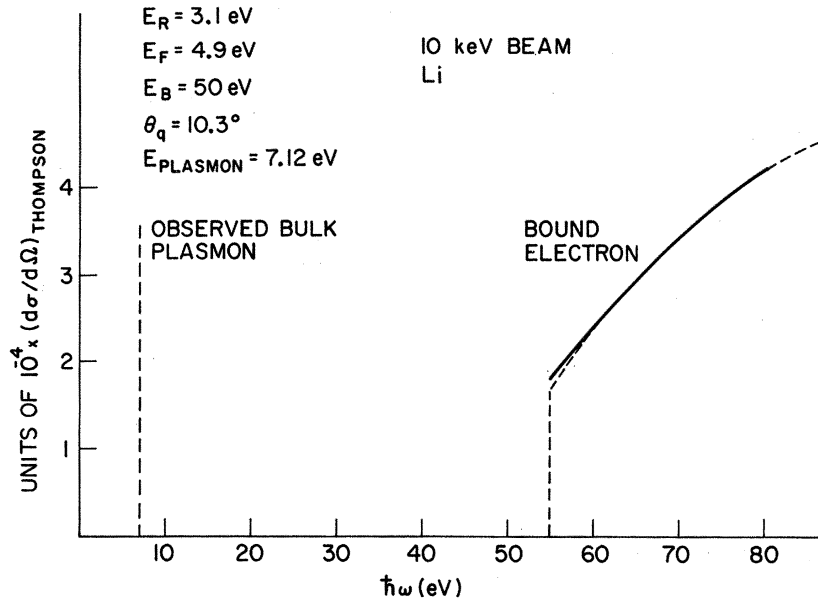


FIG. 3. Predicted x-ray Raman scattering in Li at a near forward angle. We have made use of the phase shifts calculated by Ausman and Glick (Ref. 6). The scattering has been arbitrarily fitted to the density of states, away from the edge singularity region. The inhibition of the edge in the soft x-ray spectrum has already been cancelled out at $\theta = 10^\circ$.

from the orthogonalization of the *plane wave* at the Fermi surface to the core state. As the Raman scattering angle varies, the magnitude of the momentum transfer \vec{q} changes and the coefficients $A_l(\vec{q})$ start changing their relative magnitudes.

For small q , compared to the radius of the core state, the spherical Bessel functions in Eq. (21) may be expanded. The leading term in the expansion of the $l=0$ term is of order q^4 as a result of the orthogonalization of the conduction electrons to the core s state, while the dominant term at small q is the $l=1$ state for which $A_1(\vec{q})$ varies as q^2 . A_0 ,

A_2 , and higher terms vary as q^4 or higher powers. Thus in the forward scattering direction, the threshold singularity is essentially that of the soft x-ray absorption and emission.

IV. RAMAN SCATTERING AT FINITE ANGLES

As q is increased the term in Eq. (20) which becomes strongest is the $l=0$ term. This is shown in Fig. 2 where we plot a numerical evaluation of $A_l(q)/q^2$ for $l=0, 1$, and 2. The lattice constant a for Li is 3.50 Å while the hydrogenic s core state was taken to be of the form

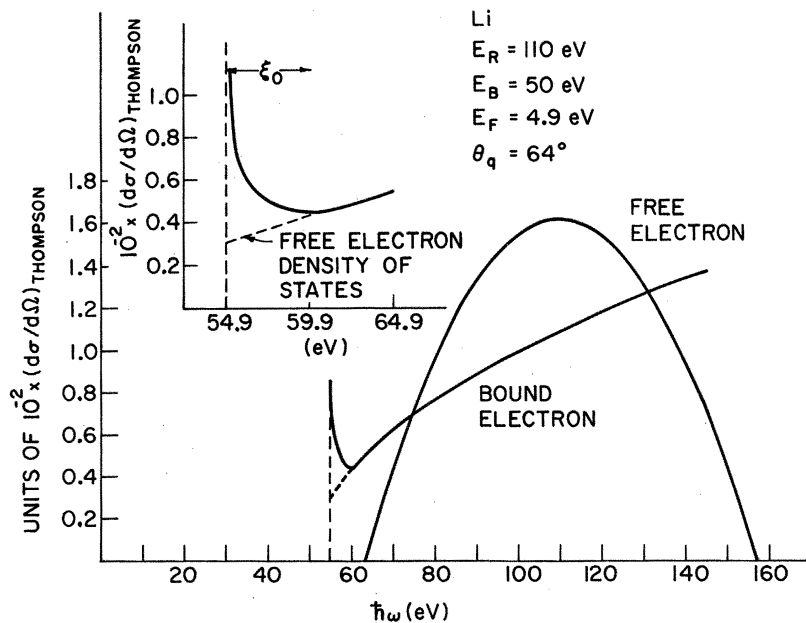


FIG. 4. As in Fig. 3. This figure shows the change in the character of the threshold singularity from inhibition for forward scattering to enhancement for finite momentum transfer. The inset is a close-up of the edge shape. The dashed curves gives the one-body contribution.

$$\Phi_{\text{core}}(r) = (\lambda^3/\pi)^{1/2} e^{-\lambda r}, \quad (23)$$

with⁸

$$\lambda = 1/a_{L1} = 5.15 \text{ \AA}^{-1}.$$

It is clear from an examination of the results shown in Fig. 2 that, as the scattering angle is increased, the behavior of the scattering cross section as a function of energy should change over from that predicted for the $l=1$ phase shift in Eq. (19) to that predicted for the $l=0$ phase shift.

This changeover for Li is plotted in Figs. 3 and 4 where we have used the phase shift estimates of Ausman and Glick.⁶ We have also plotted the free-electron Compton cross section in the same units [of Thompson cross section $(d\sigma/d\Omega)_{\text{Th}}$] as given in Ref. 7. Thus it may be seen that effects at threshold which operate in soft x-ray emission and also to some extent in the near-forward-direction Raman scattering (Fig. 3) change dramatically as the scattering angle is increased (Fig. 4) to a threshold singularity behavior such as that seen in Na near an L -band threshold.

In the calculation of the curves in Figs. 3 and 4 we have set

$$S(\vec{q}, \omega) = \rho(\omega)\theta(\omega > E_{\text{edge}})A_0(\vec{q})(\xi/\omega)^{\alpha_0} + A_1(\vec{q})(\xi/\omega)^{\alpha_1}, \quad (24)$$

with $\alpha_0 = 0.41$, $\alpha_1 = -0.1$, and neglected A_2 and higher effects which are small corrections.⁶ The parameter ξ measuring the scale over which the many-body effects occur has arbitrarily been set to equal 5 eV, which is roughly consistent with the observed inhibition of the edge in the Li soft x-ray data (neglecting lifetime effects). The dashed curves show the behavior of the noninteracting Raman cross section which in the absence of band-structure corrections is given by

$$S^0(\vec{q}, \omega) = \rho(\omega)\theta(\omega > E_{\text{edge}})[A_0(\vec{q}) + A_1(\vec{q})]. \quad (25)$$

It should be noticed that Eq. (24) is an asymptotic expansion, hence the curves of Figs. 3 and 4 are only accurate very close to threshold. For large ω they have been adjusted to follow a density-of-states behavior. Finally, we have not included any lifetime effects associated with recombination of the hole so that the infinity (zero) in the theoretical curves will be rounded off somewhat in the experiment.

In order to clearly observe the Raman edge one must contend with the presence of a Compton scattering "background" from the conduction electrons.

For the angles chosen, this Compton background does not interfere with the edge. At the small scattering angles the free-electron Compton spectrum ($q/q_F \ll 1$) due to screening effects in the electron gas is a sharp line displaced from the input x-ray energy by the plasma energy ($\hbar\omega = \hbar\omega_p = 7.1$ eV). The Raman threshold is clearly isolated. Unfortunately, it is rather weak.

As the scattering angle is increased, the intensity near threshold increases (see the Appendix in Ref. 7); however, the dip quickly becomes a peak. The rapid changeover is directly connected to the smallness of the parameter $k_F a_{L1}$. The scattering of an electron at the Fermi surface is almost pure s wave except in the extreme forward direction where the orthogonality of the initial and final wave functions suppresses the s -wave scattering. The observation of the dip will be difficult. The presence or absence of a peak at larger angles will either confirm or disprove the conjecture concerning the origins of the soft x-ray anomaly in Li.

V. CONCLUDING REMARKS

We have proposed that a Raman scattering experiment could be used to investigate the properties of the soft x-ray threshold in metals. An analysis for the case of Li metal suggests that the character of the many-body contributions to the scattering should change dramatically as the angle of the experiment is increased away from the forward direction.

In addition to the added information obtained in the Raman scattering experiment, such a hard x-ray process has several purely experimental advantages over a soft x-ray emission or absorption experiment. First, it is a bulk process, i. e., the 10-keV x rays penetrate a low- Z material such as Li to distances approximating 1 cm. In contrast, soft x-ray penetration lengths are in the few-hundred \AA range so that surface preparation is a real problem. In a hard x-ray Raman process one can easily use bulk single crystals and one can quite conveniently vary the temperature. Both of these features are difficult to obtain in a soft x-ray emission experiment. The real difficulty in the hard x-ray Raman process lies in the question of energy resolution.⁹ In the Raman process we are forced to analyze small energies of the order of a few tenths of an eV on a scale of 10 keV. Such resolutions are difficult to reach but we believe they can be achieved.

*Research partly supported by Army Research Office, Durham, North Carolina.

†AEC Predoctoral Fellow.

¹See, for example, A. J. McAlister, Phys. Rev. **186**, 595 (1969), and references mentioned therein.

²R. S. Crisp and S. E. Williams, Phil. Mag. **5**, 525 (1960).

³R. S. Crisp and S. E. Williams, Phil. Mag. **6**, 365 (1961).

⁴G. D. Mahan, Phys. Rev. **163**, 612 (1967).

⁵P. Nozières and C. de Dominicis, *Phys. Rev.* **178**, 1097 (1969); B. Roulet, J. Gavoret, and P. Nozières, *ibid.* **178**, 1072 (1969).

⁶G. A. Ausman and A. J. Glick, *Phys. Rev.* **183**, 687 (1969).

⁷See, for example, P. M. Platzman and N. Tzoar, *Phys. Rev.* **139**, 410 (1965).

⁸J. C. Slater, *Solid State Physics* (McGraw-Hill, New York, 1967).

⁹See, for example, the data of T. Suzuki, T. Kishimoto, and T. Kaji, *J. Phys. Soc. Japan* **29**, 730 (1970). Their Raman scattering data from light elements probably does not resolve the effects of the present paper.

PHYSICAL REVIEW B

VOLUME 4, NUMBER 10

15 NOVEMBER 1971

Coherent-Potential Approximation for Alloys with Random Off-Diagonal Elements*

E-Ni Foo

Department of Physics, Drexel University, Philadelphia, Pennsylvania 19104
and Department of Physics, Temple University, Philadelphia, Pennsylvania 19122

and

H. Amar and M. Ausloos

Department of Physics, Temple University, Philadelphia, Pennsylvania 19122
 (Received 19 October 1970)

The single-site coherent-potential approximation for substitutional disordered alloys is extended to include the effects of random off-diagonal elements and of the formation of clusters. Our results are in good agreement with the exact numerical computations performed on a one-dimensional system over most of the energy region.

I. INTRODUCTION

Recently, the one-electron theory of disordered binary alloys has been studied most intensively. Because of the lack of crystal symmetry in disordered alloys, their properties evaluated by statistical averages over all configurations are difficult to calculate. Therefore various approximations have emerged. The virtual crystal¹ and the *t*-matrix² approximations are the conventional approaches. More recently the coherent-potential approximation (CPA)³⁻⁵ has been shown to be the most powerful method to treat the disordered alloys. It is a self-consistent method which serves as an interpolating scheme for the entire range of concentrations and scattering strengths in disordered alloys.

The CPA is developed within the framework of multiple scattering theory introduced by Lax.⁶ Soven³ and Taylor⁴ first used the CPA to calculate the electronic density of states (EDS) and the phonon spectrum in disordered substitutional binary alloys. They introduced the concept of a coherent potential which, when placed on every site of the alloy lattice, will simulate the EDS or the phonon spectrum of the actual alloy, respectively. To determine the coherent potential, one generally requires that a single scatterer imbedded in this effective medium should produce no further scattering on the average. A detailed discussion of the CPA can be found in Velický *et al.*⁵ This theory,

based on a single-site approximation (SCPA), suffers from three major drawbacks: (i) its failure to produce a tail in the edge of the density of states, (ii) its restriction to alloys with composition independent off-diagonal elements, and (iii) its neglect of the effects due to the formation of clusters. The first point has been discussed by Eggarter *et al.* using a percolation theory⁷ and by Schwartz using an extended CPA,⁸ which includes the effects due to pairs at all distances, but excludes effects of random off-diagonal elements. The second point has been treated by Soven in the CPA for a system of muffin tin potentials,⁹ in which the pure constituents have different bandwidths, and by Blackman *et al.* using the CPA in a locator expansion¹⁰ in which the effects of clustering have not been considered. The third point has been discussed by Freed *et al.* in a cluster theory,¹¹ in which there is an infinite hierarchy of equations of motions [in which the *n*-atom Green's functions are coupled to the (*n*+1)-atom Green's function] and which provides an improvement over the SCPA and becomes more and more accurate by inclusion of larger and larger clusters. One problem is to know the optimum size of clusters convenient for machine computation and for reproducing the features of the true spectra at the same time. The SCPA corresponds to truncation in the equation of motion of a 1-atom Green's function. Berk¹² has considered the last two points in the weak-coupling limit. Montgomery *et al.*¹³ have treated amorphous